INTERNATIONAL JOURNAL OF ELECTRONICS AND COMMUNICATION ENGINEERING &TECHNOLOGY [IJECET]

ISSN Print: 0976-6464 / ISSN Online: 0976-6472

High Quality Peer Reviewed Refereed Scientific, Engineering & Technology, Medicine and Management International Journals

PUBLISHED BY

IAEME Publication

Plot: 03, Flat- S 1, Poomalai Santosh Pearls Apartment,
Plot No. 10, Vaiko Salai 6th Street, Jai Shankar Nagar, Palavakkam, Chennai - 600 041,
Tamilnadu, India
E-mail : editor@iaeme.com, ieamedu@gmail.com
www.iaeme.com

International Journal of Electronics and Communication Engineering and Technology (IJECET)
Volume 16, Issue 2, May-August 2025, pp. 36-59, Article ID: IJECET_16_02_003
Available online at https://iaeme.com/Home/issue/IJECET?Volume=16&Issue=2
ISSN Print: 0976-6464; ISSN Online: 0976-6472; Journal ID: 3587-7166
Impact Factor (2025): 13.44 (Based on Google Scholar Citation)
DOI: https://doi.org/10.34218/IJECET_16_02_003

A TWO-STAGE DEEP LEARNING FRAMEWORK FOR AUTOMATED GLAUCOMA DETECTION USING U-NET AND CNN ENSEMBLES

Dr. S. N. Nisha Rani
Professor, Department of Electronics and Communication Engineering,
Fatima Michael College of Engineering and Technology, Madurai-20, India.

Mrs. R. Nagadeepa
Assistant Professor, Department of Electronics and Communication Engineering, Fatima Michael College of Engineering and Technology, Madurai-20, India.

Mrs. P. Jebane
Assistant Professor, Department of Electronics and Communication Engineering, Fatima Michael College of Engineering and Technology, Madurai-20, India.

Mr. M. Elayaraja
Associate Professor, Department of Electronics and Communication Engineering, Fatima Michael College of Engineering and Technology, Madurai-20, India.

ABSTRACT

Glaucoma is a leading cause of irreversible blindness worldwide, often progressing asymptomatically until advanced stages, making early detection critical yet challenging. Conventional screening methods are largely subjective, time-intensive, and reliant on skilled ophthalmologists, whose availability is limited in densely populated regions such as India. To address these limitations, we propose a two-stage *automated glaucoma screening system. In the first stage, the optic disc is segmented using a U-Net-based deep learning architecture. In the second stage, glaucoma classification is performed using both pretrained deep convolutional neural networks (CNNs) and a customized CNN model. Despite existing advancements, challenges such as inconsistent image quality, segmentation errors affecting cup-to-disc ratio (CDR) estimation, and limited model generalizability persist. This study addresses these gaps by improving segmentation accuracy and classification precision through an ensemble learning approach that integrates both pretrained and customized CNN models. Experimental evaluation on the DRISHTI-GS1 dataset demonstrates that the proposed ensemble model achieves a classification accuracy of 96%, outperforming conventional methods. Additionally, the CDR computed from the segmented optic cup and disc serves as a valuable reference metric to support early-stage glaucoma diagnosis by clinicians.*

Keywords: Glaucoma, CNN, CDR, Segmentation.

Cite this Article: S. N. Nisha Rani, R. Nagadeepa, P. Jebane, M. Elayaraja. (2025). A Two-Stage Deep Learning Framework for Automated Glaucoma Detection Using U-Net and CNN Ensembles. *International Journal of Electronics and Communication Engineering and Technology (IJECET)*, 16(2), 36–59.

DOI: https://doi.org/10.34218/IJECET_16_02_003

I. Introduction

Glaucoma is a leading cause of irreversible blindness, with global projections estimating that approximately 111.8 million people will be affected by 2040, particularly in Asia and Africa. Early detection is critical to preventing vision loss; however, the disease is often asymptomatic in its initial stages, which significantly delays diagnosis and treatment. Traditional image processing and machine learning techniques—such as the Glaucoma Risk Index proposed by Bock et al. (2010), fractal dimension analysis by Kolář and Jan (2008), and adaptive threshold-based image processing by Issac et al. (2015)—have contributed to automated glaucoma detection. Nevertheless, these methods rely heavily on handcrafted feature extraction, limiting their scalability and general applicability.A key biomarker for glaucoma diagnosis is the cup-to-disc ratio (CDR), which depends on the accurate segmentation of the optic disc and cup. Various methods have been proposed to improve this segmentation, including superpixel classification (Cheng et al.), multi-parametric segmentation (Rehman et al., 2013), and structural detection approaches (Chrástek et al., 2005). While these methods have enhanced segmentation accuracy, they still face challenges related to overlapping anatomical structures and variable image quality.Recent advances in deep learning have shown promise in addressing these limitations. Studies by Chen et al., Serte and Serener (2015, 2019) demonstrate the effectiveness of convolutional neural networks (CNNs) in glaucoma screening. However, deep learning models still struggle with issues of explainability, generalizability, and dataset diversity, which hinders their clinical translation. To overcome these barriers, hybrid models integrating CNNs with additional techniques have been explored. For instance, works by Salam et al., Koh et al. (2016, 2018), and others have aimed to improve detection accuracy, although challenges in standardization and clinical validation remain.To address these gaps, a multi-modal glaucoma detection system has been proposed, leveraging both clinical biomarkers and retinal fundus images. This system utilizes advanced deep learning architectures to enable comprehensive feature extraction. Three hybrid models have been developed: (1) a combination of Vision Transformers (ViT) and Residual Networks (ResNet), (2) an integration of Object-Window-Location Vision Transformers (OWL-ViT) with ResNet to enhance global contextual understanding, and (3) a fusion of Hierarchical Swin Transformers (with Shifted Windows) and ResNet. Among these, the third model demonstrated the highest performance, as reported by Rishikesh Sivakumar (2025), highlighting its potential for robust and accurate glaucoma detection in diverse clinical environments.

A. Glaucoma Detection Methods:

Doctors leverage computer-aided systems to diagnose glaucoma by analyzing retinal images that capture the back of the eye. Recognizing specific visual indicators of the disease within these images is critical for accurate diagnosis. Several imaging modalities are available for capturing the retina, including 2D color fundus photographs, 3D optical coherence tomography (OCT), red-free imaging, fluorescein angiography, scanning laser ophthalmoscopy, and cross-sectional imaging techniques. Among these, standard 2D fundus photographs are the most widely used in clinical practice due to their low cost, accessibility, and compatibility with automated image analysis algorithms.

The procedure of capturing these images is referred to as ophthalmoscopy or funduscopy. Once fundus images are obtained, they are processed using computer vision and deep learning techniques to identify hallmark signs of glaucoma progression. Two primary indicators are typically assessed: (1) retinal nerve fiber layer (RNFL) thinning, which indicates damage to the nerve fibers, and (2) the cup-to-disc ratio (CDR), which measures the relative size of the optic cup to the optic disc. A higher CDR often correlates with glaucomatous damage.

Figure 1 illustrates the diagnostic workflow involving fundus image acquisition and computer-assisted analysis for glaucoma screening.

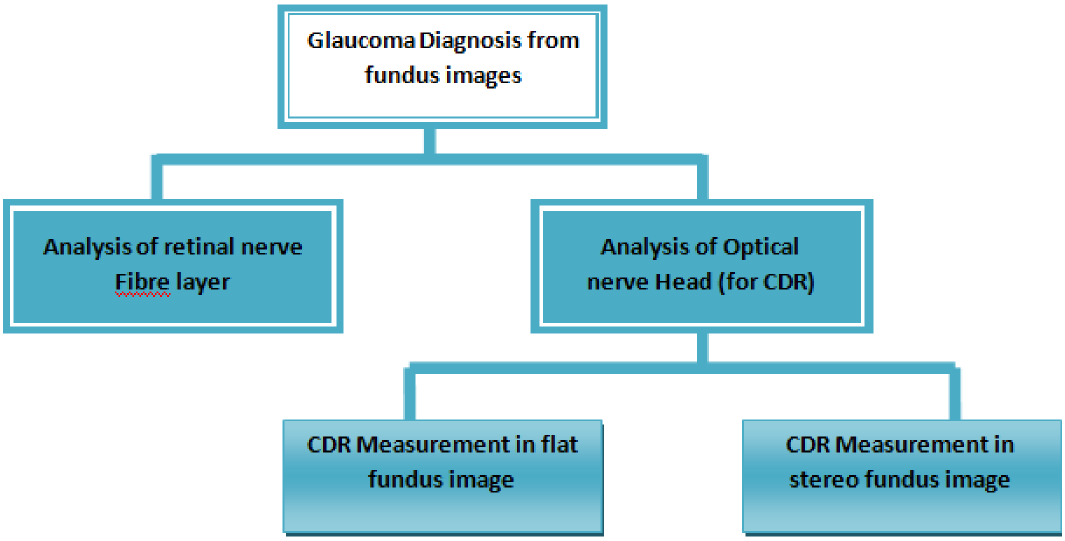

Figure 1: Glaucoma Screening Methods

II. Existing work

Glaucoma is a progressive optic neuropathy characterized by irreversible damage to the optic nerve, commonly associated with elevated intraocular pressure (IOP). As the disease is typically asymptomatic in its early stages, early detection and timely intervention are critical to prevent permanent vision loss. Unfortunately, many individuals are diagnosed only at an advanced stage, by which time substantial and often irreversible visual impairment has already occurred.Routine screening plays a pivotal role in early detection and effective management of glaucoma. However, conventional diagnostic methods—such as intraocular pressure measurement, visual field analysis, and Optical Coherence Tomography (OCT)—are often subjective, time-consuming, and reliant on expensive equipment and skilled personnel. These requirements make widespread screening particularly difficult, especially in underserved or remote regions with limited access to ophthalmic care. As a result, diagnosis and treatment are frequently delayed, exacerbating the risk of vision loss in affected populations.

III. Proposed Work

To achieve high accuracy and efficiency in glaucoma detection, we propose an automated two-stage deep learning framework. In the first stage, the **optic disc (OD)** is accurately localized and segmented from retinal fundus images using the **U-Net architecture**. U-Net's encoder–decoder design is particularly effective for biomedical image segmentation, as it captures both contextual and spatial features, enabling the generation of high-resolution segmentation masks. Accurate OD isolation is critical at this stage, as it minimizes interference from surrounding retinal structures, thereby enhancing the precision of subsequent analysis.

In the second stage, the segmented OD region is evaluated using three distinct deep Convolutional Neural Network (CNN) architectures for glaucoma classification. The first model employs a conventional deep learning approach to extract structural and textural features for distinguishing glaucomatous eyes from healthy ones. The second model applies transfer learning using pretrained networks such as ResNet, VGG, or Inception, leveraging knowledge from large-scale datasets to improve performance on relatively smaller glaucoma datasets. The third model incorporates a hybrid CNN with an attention mechanism, enabling the network to focus on the most relevant regions of the optic disc, suppress background noise, and enhance classification sensitivity.

To further improve the robustness and reliability of the system, the outputs from these CNN models are combined using ensemble techniques, such as weighted averaging or majority voting. This fusion strategy enhances predictive performance by leveraging the complementary strengths of the individual models. By isolating the OD prior to classification, the framework ensures that the models concentrate solely on clinically significant regions, thus reducing false positives and improving diagnostic accuracy.

The integration of multiple CNN architectures and attention-based mechanisms improves the system's generalization capability across diverse imaging conditions. This fully automated approach facilitates scalable, cost-effective glaucoma screening, especially in resource-constrained environments. By reducing dependence on expert intervention, the proposed system enables earlier diagnosis and timely treatment—key factors in preventing glaucoma-induced vision loss.

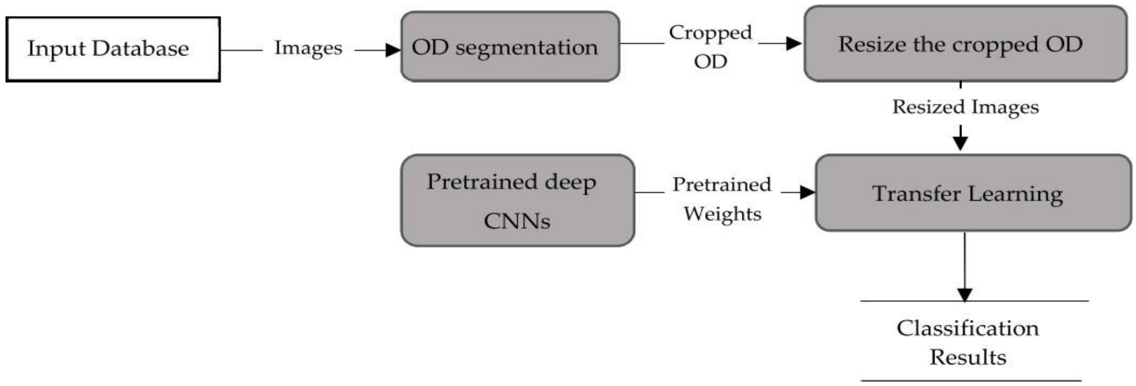

Figure 2: Two-Stage Deep Learning Framework for Automated Glaucoma Detection

A. Glaucoma Classification:

The relationship between the optic disc and the cup is measured by the Cup-to-Disc Ratio (CDR) which is a crucial criterion in the classification of glaucoma. The CDR usually increases as the disease worsens. Using retinal fundus images our methodology employed the VGG16 Convolutional Neural Network (CNN) model to distinguish between glaucomatous and non-glaucomatous cases. The 16-layer deep architecture of the VGG16 model is well known for its ability to extract hierarchical features from images allowing for accurate and trustworthy classification.

Additionally glaucoma severity was categorized using CDR values: CDR values between 0.3 and 0.5 were considered mild glaucoma those between 0.5 and 0.8 were considered moderate glaucoma and those greater than or equal to 0.8 were considered severe glaucoma. Early intervention and customized treatment plans are made possible by this stratification which provides insightful information about the stage of disease progression. Our approach improves patient outcomes by automating the screening process increasing diagnostic accuracy and facilitating large-scale glaucoma detection by fusing deep learning with CDR-based classification.

Glaucoma severity can also be classified from cup to disc ratio:

Mild (CDR >0.3 = < 0.5)

Moderate (CDR >=0.5 and < 0.8)

Severe (CDR >= 0.8)

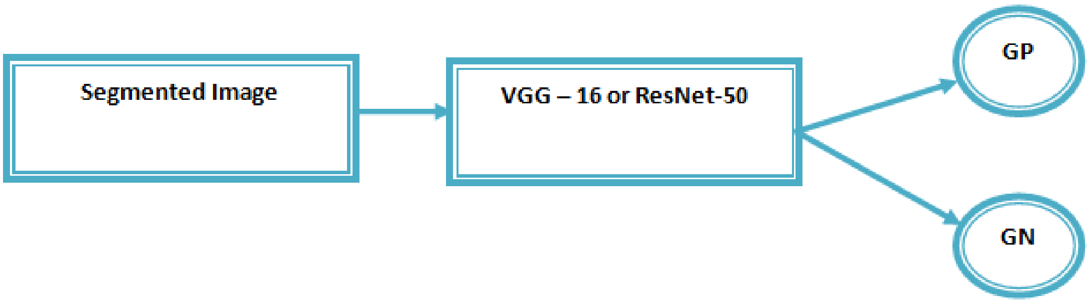

Figure 3: Glaucoma Classification Using Deep CNN Models

B. OD/OC Segmentation Using UNet:

The proposed model architecture utilizes an encoder-decoder framework optimized for precise segmentation of the optic cup and optic disc, which are essential for calculating the Cup-to-Disc Ratio (CDR)—a critical biomarker for glaucoma diagnosis.

The encoder comprises four parallel atrous (dilated) convolutions with varying dilation rates to effectively capture multi-scale contextual features. These features are then fused using average pooling applied to the final feature map, ensuring comprehensive spatial information aggregation. To enhance the feature representation and reduce the computational burden, a 1×1 convolution is applied to decrease the number of channels while preserving important information.

The decoder is designed to reconstruct fine object boundaries encoded by the CNN. Initially, the encoded features are bilinearly upsampled by a factor of four and then concatenated with corresponding low-level features from earlier layers. Since these low-level features often contain a high number of channels, a 1×1 convolution is used to selectively retain the most relevant information. Subsequently, a 3×3 convolution is applied to refine the feature maps, followed by another bilinear upsampling by a factor of four to achieve the final output resolution.

This decoder essentially reverses the encoder operations, reconstructing the spatial structure while integrating both low- and high-level features. The key operations in this architecture—downsampling during encoding and upsampling during decoding—enable the model to preserve semantic context and boundary precision.

By segmenting both the optic disc (OD) and optic cup (OC) regions, the system accurately computes the CDR, which serves as a valuable quantitative parameter for assisting ophthalmologists in early glaucoma detection and monitoring disease progression.

C. Classification of Normal and Glaucoma Retinal Images Using Ensemble CNN:

The core principle of ensemble learning closely resembles the decision-making process in clinical glaucoma screening. In practice, when an ophthalmologist encounters uncertainty in a diagnosis, they may consult other specialists to obtain a more reliable conclusion. Similarly, our ensemble-based approach aggregates predictions from multiple individual CNN models—analogous to consulting several ophthalmologists—to arrive at a unified decision, thereby reducing the overall generalization error and enhancing diagnostic robustness.

Empirical evidence suggests that ensemble Convolutional Neural Networks (CNNs) outperform individual CNN models in terms of both accuracy and reliability. In this study, Method P1 employs a transfer learning scheme utilizing pretrained deep CNNs. These models were originally trained on the ImageNet dataset, which contains millions of labeled images across thousands of object categories. To tailor these models for glaucoma classification, the segmented optic disc (OD) regions were resized to match the input dimensions of each pretrained CNN. Each resized image was then independently passed through multiple CNN architectures.

To adapt the pretrained networks to our task, the final fully connected (FC) layer in each model was replaced with a new output layer suitable for binary classification (normal vs. glaucomatous). This layer was subsequently fine-tuned using the labeled OD images from the glaucoma dataset. During training, the cross-entropy loss function was minimized iteratively to optimize model performance and improve classification accuracy.

$$CE(Y, Y^{Predict})=\sum_{C=1}^{2}\binom{n}{k}x^{k}a^{n-k}\,[Y\log(Y_c^{Predict})+(1-Y_c)\log(1-Y_c^{Predict})] \longrightarrow (1)$$

A customized CNN model is developed to classify glaucoma and normal images, in order to improve generality of the proposed model a tiny and efficient model proposed to use segmented image.

IV. Experiment and Discussion

The Drishti-GS1 dataset was utilized for training and evaluating the proposed glaucoma detection system. This publicly available dataset comprises a total of 101 retinal fundus images, which were originally divided into 50 training images and 51 testing images. Each image was independently annotated by four ophthalmologists with varying levels of clinical expertise to ensure reliability and diagnostic consistency. Glaucoma cases were identified by clinical investigators based on comprehensive ophthalmic examinations conducted during the patients' visits. The patient cohort included individuals aged between 40 and 80 years, with an approximately equal distribution of males and females.To address the limitations of dataset size and improve the generalization capability of the model, various data augmentation techniques were applied. These included horizontal and vertical flipping, rotation, and zoom transformations, effectively increasing the dataset size from 101 to 524 images. From this augmented dataset, 455 images (80%) were allocated for model training, while the remaining 64 images (20%) were used for model testing. This augmentation strategy ensured a more robust training process and reduced the risk of overfitting, particularly in a deep learning context.

A. Evaluation Metrics

To assess the performance of the proposed system, different evaluation metrics were employed for classification and segmentation tasks.

1. Classification Metrics

For glaucoma classification, the following metrics were used:

- **Accuracy**: Measures the overall correctness of the model's predictions.

$$Accuracy = \frac{TP + TN}{TP + TN + FP + FN}$$

- **Precision**: Indicates the proportion of positive identifications that were actually correct.

$$Precision = \frac{TP}{TP + FP}$$

- **Recall (Sensitivity)**: Measures the proportion of actual positives that were correctly identified.

$$Recall = \frac{TP}{TP + FN}$$

2. Segmentation Metrics

For evaluating the quality of optic disc (OD) and optic cup segmentation, the following metrics were utilized:

- **Dice Coefficient (F1 Score)**: Measures the overlap between the predicted and ground truth segmentations.

$$Dice = \frac{2TP}{2TP + FP + FN}$$

- **Intersection over Union (IoU)**: Calculates the ratio of the intersection to the union of predicted and ground truth segmentations.
-

$$IoU = \frac{TP}{TP + FP + FN}$$

Where

True Positive (TP): Number of correctly predicted OD pixels.

True Negative (TN): Number of correctly identified non-OD pixels.

False Positive (FP): Number of non-OD pixels incorrectly identified as OD pixels.

False Negative (FN): Number of OD pixels incorrectly identified as non-OD pixels.

B. Model Training setup

The proposed model was implemented using the TensorFlow framework and GPU acceleration for enhanced computational efficiency. The training process employed the Adam optimizer, with an initial learning rate of 0.001 and a mini-batch size of 16. To prevent overfitting, a weight decay constant of 10−5 was applied. The learning rate was scheduled to decay by a factor of 0.1 after every 30 epochs.During training, the model's two branches were updated alternately in each iteration, enabling a collaborative optimization process until the synergic network converged. The training phase consisted of a total of 40 epochs.In the testing phase, input images were passed through the trained model, and predictions were generated based on the Softmax probability distribution at the output layer. The class with the highest Softmax score was selected as the final prediction, enabling accurate classification of glaucomatous and non-glaucomatous cases.

C. Performance analysis of the proposed model

The segmentation and classification performance of the proposed deep learning model was compared against existing handcrafted feature-based models, which utilize traditional machine learning techniques for segmenting the optic disc (OD) and optic cup (OC). These conventional approaches often rely on manually engineered features, which may limit their generalizability and accuracy in diverse imaging conditions.In contrast, our proposed model leverages end-to-end learning to automate both segmentation and classification tasks, yielding superior performance. To quantitatively assess classification performance, a confusion matrix was generated, as presented in Table 1. For the segmentation evaluation, pixel-wise cross-entropy loss was employed as the objective function, providing a fine-grained measure of the model's ability to accurately distinguish between anatomical regions at the pixel level.This comparative analysis demonstrates that the proposed model significantly outperforms traditional methods, particularly in terms of precision, recall, and overall segmentation quality.

Table 1: Confusion matrix for segmentation

Class	**OD region**	**Normal Region**
OD region(70)	56	14
Normal Region(154)	4	150

Table 2: Confusion matrix for classification

Class	**Glaucoma**	**Non-Glaucoma**
Glaucoma(44)	42	2
Non-Glaucoma(20)	3	17

The training and validation accuracy of the proposed model is shown in Figure 4

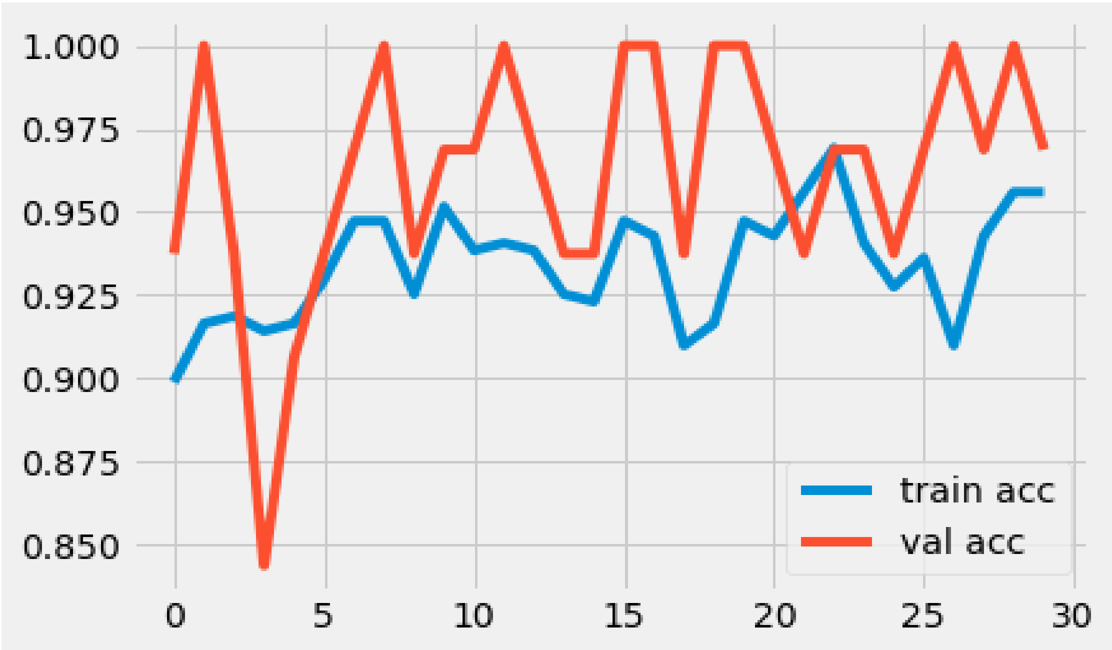

Figure 4: Training and Validation Accuracy

Figure 4 illustrates the training and validation performance of the proposed model on the **Drishti-GS1 dataset**. The **training accuracy** (depicted by the blue line) demonstrates a consistent upward trend over **30 epochs**, indicating effective convergence and successful feature learning by the model. The **validation accuracy** (shown in red) remains high and stable throughout the training process, highlighting the model's strong **generalization capability** on unseen data.This performance stability, combined with the high accuracy observed across both training and validation phases, confirms the model's **robustness and reliability** in glaucoma detection. The results are further enhanced by the application of **data augmentation techniques**, which improve the model's ability to adapt to variability in retinal images, thereby increasing its effectiveness in real-world screening scenarios.

The training accuracy (blue line) shows a steady increase over 30 epochs, demonstrating effective learning, while the validation accuracy (red line) remains consistently high, reflecting strong generalization to unseen data. The overall accuracy reflects the model's reliability in detecting glaucoma, supported by data augmentation techniques that enhance its effectiveness.

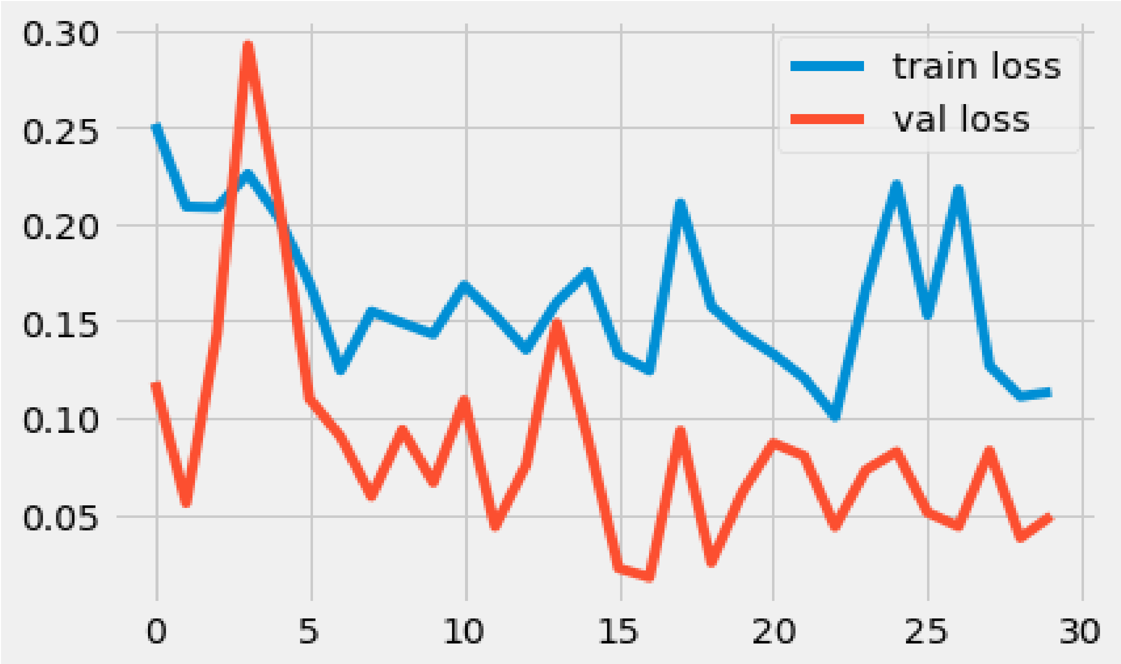

Figure 5: Training and validation loss

Figure 5 presents the training loss (blue line) and validation loss (red line) curves over the course of 30 epochs on the Drishti-GS1 dataset. Both curves exhibit a declining trend, indicating that the model is effectively learning and minimizing the loss function during training. The consistent reduction in training loss reflects the model's ability to optimize its internal parameters, while the relatively low and stable validation loss, despite minor fluctuations, suggests strong generalization performance on unseen data.

The observed behavior confirms that the model is neither overfitting nor underfitting and is capable of robust performance in glaucoma detection tasks. These results, in conjunction with the accuracy metrics, reinforce the reliability of the proposed approach in clinical and large-scale screening applications.

The performance of the proposed model with other existing method is shown in Table 3

Table 3: Overall proposed Performance (Segmentation and Classification)

Model	Classification (Accuracy)	Segmentation (DICE)	Segmentation (IoU)
Intensity based texture Feature extraction [5]	90.2	83.4	87.4
Super-pixel Segmentation [7]	92.3	85.4	86.7
Proposed Method	96	86.3	87.1

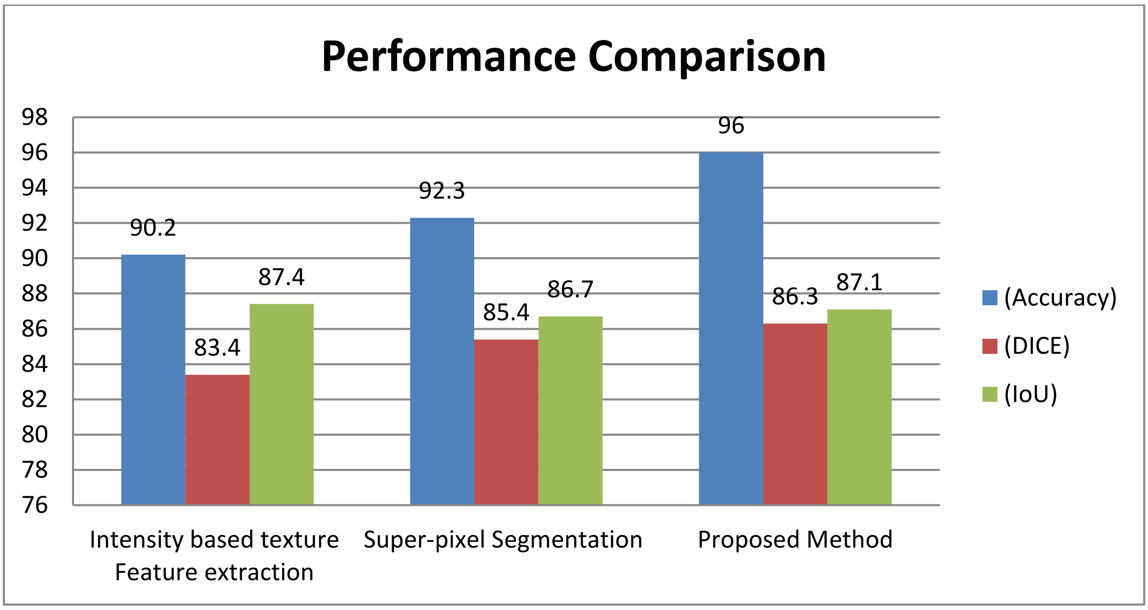

Figure 6: Overall Performance of proposed Method (Segmentation and Classification)

Table 4: Ablation study of different classifier

Model	ClassificationAccuracy
Unet+VGG-19	92
Unet+ResNet-50	94
Unet + Our Proposed CNN	94
Unet + Ensemble (Proposed+ ResNet-50)	96

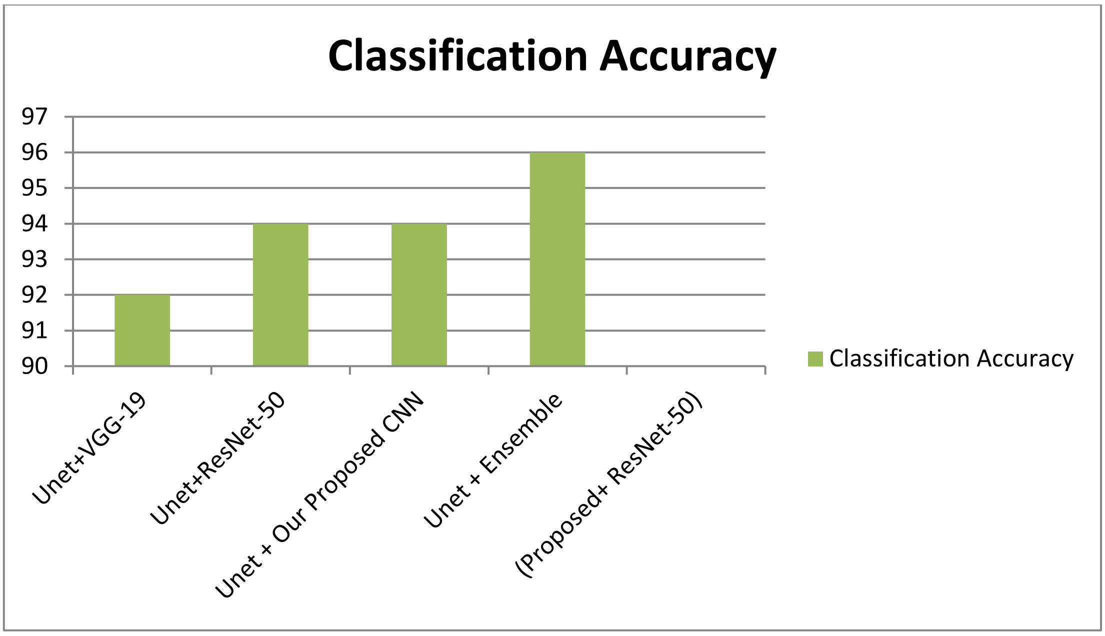

Figure 6: Performance comparison of Proposed Method

Original Image	Predicted Segmentation	Optical Disc
		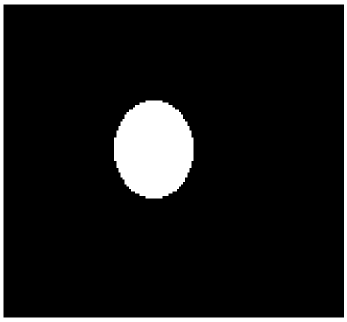
		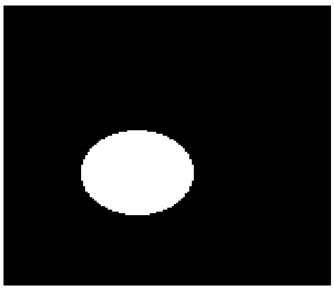

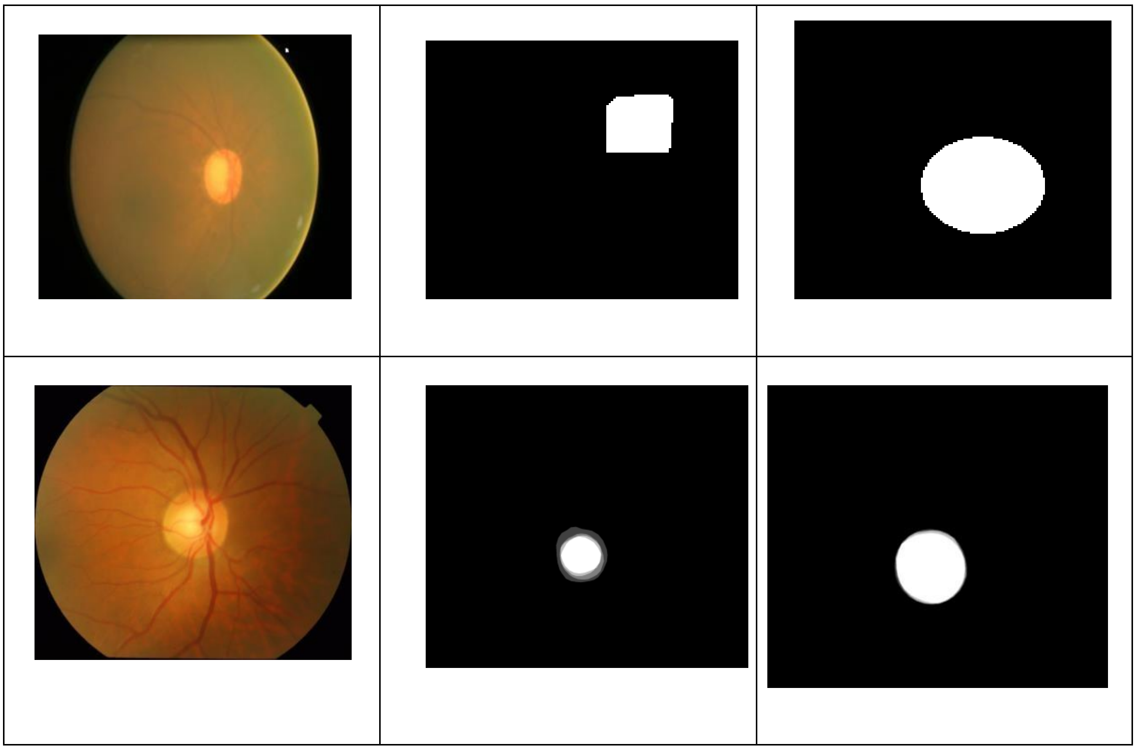

Figure 7: Sample Optic Disc Segmented Output

Along with the ground truth reference by measuring the height and weight of the segmented Optical Cup and Optical Disc, CDR (Cup Disc Ratio is calculated). This CDR is considered for additional reference for Glaucoma detection.

D. Results and Discussion

Upon conducting an analysis of the segmentation and classification efficacy of the proposed model, it is observed that its accuracy in segmenting the optic disc (OD) and optic cup (OC) is marginally superior to that of the existing handcrafted methodologies. The classification efficacy of the proposed convolutional neural network (CNN) model for the categorization of glaucoma images exhibits enhancement when compared with the pre-existing models VGG-16 and ResNet-50. It is noteworthy that the weights acquired from the pre-trained CNN model, originally designed for natural image classification, are not optimally suited for the classification of medical images. In terms of computational complexity, the proposed CNN demonstrates computational efficiency, necessitating a minimal number of floating-point operations per second (FLOPS) in comparison to the existing pre-trained CNN models.

Table 5: Confusion Matrix

	Predicted Values	
Actual Values	70	4
	3	57

The confusion matrix evaluates the model's classification performance by comparing actual and predicted values. 70 glaucoma-positive cases and 57 glaucoma-negative cases are correctly classified by the suggested model which also has very few errors (4 false positives and 3 false negatives). This outcome demonstrates the models excellent classification accuracy and dependability in identifying cases of glaucoma.

The models performance in segmentation and classification tasks is indicated by its accuracy and Dice score. In figure 8 the suggested model surpasses alternative techniques like handcrafted-based clustering and U-Net–VGG-16 with an accuracy of 94% and a Dice score of 0. 91. This enhancement shows that the suggested model performs better in terms of segmentation and classification for the detection of glaucoma.

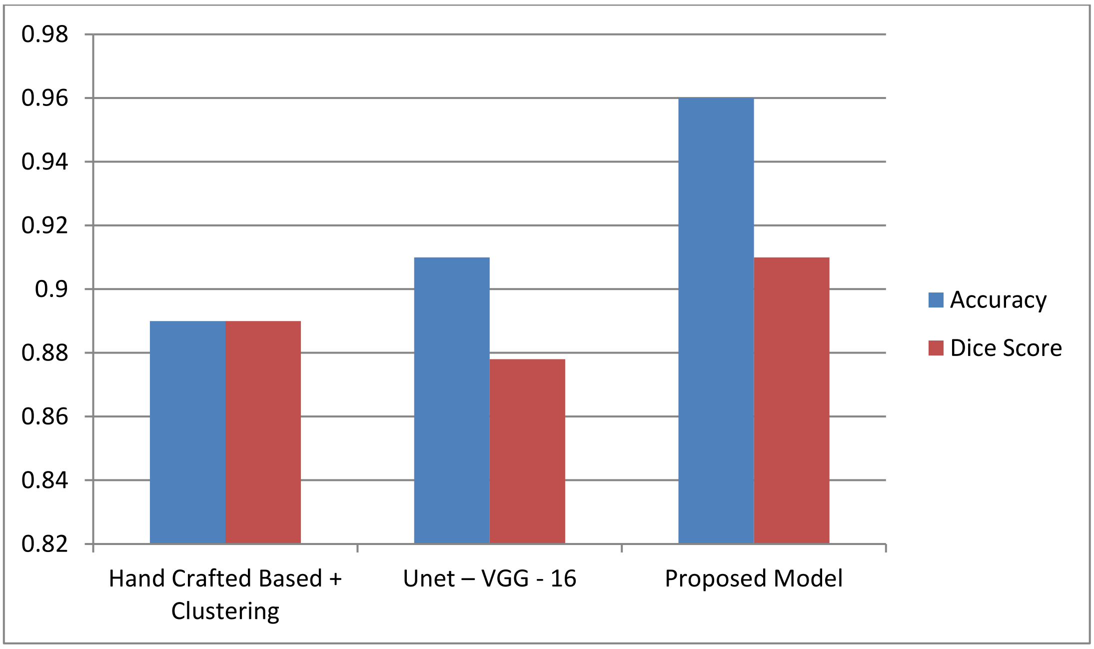

Figure 8: Accuracy and Dice Score Comparison

One important measure of glaucoma is the Cup-to-Disc Ratio (CDR) which is used to assess the classification accuracy across various images. The suggested models ability to correctly classify glaucoma-positive and negative cases is demonstrated by the close match between its predicted CDR values and the actual ground truth values. For clinical applications the model is extremely dependable due to its high consistency.

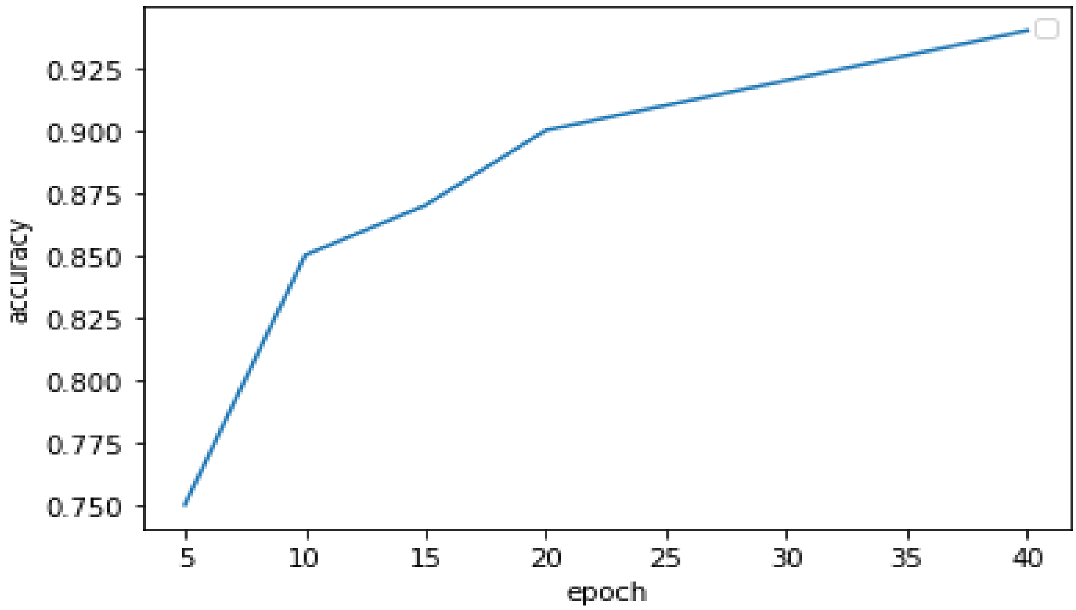

Figure 9: Testing classification of Accuracy vs Epoch

The learning efficiency of the suggested model was assessed by analyzing its classification accuracy across several training epochs. From figure 9 Accuracy varies at first as the model picks up important features from the dataset but as the number of epochs rises accuracy gradually gets better because of weight optimization and error reduction. The model has achieved its peak performance without overfitting when the accuracy eventually stabilizes. This pattern demonstrates that given enough training epochs the suggested model learns from data efficiently and attains higher classification accuracy.

Table 6: CDR Value with Ground Truth

Image No.	Image	CDR	Ground Truth	Class
ARI_0036	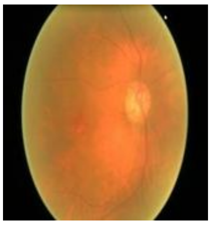	0.875	0.91	Glaucoma Positive
ARI_0078		0.855	0.88	Glaucoma Positive
ARI_0045		0.21	0.18	Glaucoma Negative

Because it measures the proportional size of the optic cup to the optic disc the Cup-to-Disc Ratio (CDR) is an essential diagnostic tool for glaucoma. A higher CDR usually means that glaucoma is more likely to occur. In order to assess the suggested model actual ground truth values gathered from medical specialists were compared to its predicted CDR values. By consistently producing CDR predictions that closely match the ground truth the model reduces the disparities seen in earlier approaches as the results show. The suggested method for automated glaucoma screening and diagnosis is more reliable due to the accuracy of the CDR estimation. Additionally the models capacity to maintain a low margin of error in CDR estimation suggests that it may find use in clinical settings lessening the need for ophthalmologists to perform manual evaluations.

VI. Conclusion

We present an effective technique that significantly enhances the segmentation and classification accuracy of the optic disc (OD) and optic cup (OC) regions in retinal fundus images, thereby facilitating more accurate glaucoma classification. The proposed architecture is built upon the U-Net Convolutional Neural Network (CNN), which is well-suited for biomedical image segmentation and is employed here to accurately delineate the OC and OD regions. Specifically, our model attained a classification accuracy of 96% and a Dice similarity score of 0.91 for segmentation, indicating its robustness and reliability.

Despite these promising results, the development of more extensive glaucoma image repositories and advanced network architectures remains critical. Since deep learning models rely heavily on large volumes of labeled data, expanding datasets would further improve classification accuracy—especially for ambiguous or subtle lesion cases. This also opens avenues for future research into automated lesion localization and improved clinical decision support systems.

References

[1] R. Bock, J. Meier, L. G. Nyl, G. Michelson, “Glaucoma risk index: automated glaucoma detection from color fundus images,” Medical Image Analysis, vol. 14, pp. 471–481, 2010.

[2] Anitha J, Vijila CKS, Hemanth DJ. An overview of computational intelligence techniques for retinal disease identification applications. Int J Rev Comput. 2009;5: 29–46.

[3] E. Dervisevic, S. Pavljasevic, A. Dervisevic, S.S. Kasumovic, “Challenges In Early Glaucoma Detection,” Med Arch., vol. 70, pp. 203–207, June 2016.

[4] Rishikesh Sivakumar, Anita PencovaEnhancing glaucoma detection through multi-modal integration of retinal images and clinical biomarkers.Volume 143, 1 March 2025, 110010 https://doi.org/10.1016/j.engappai.2025.110010

[5] Rajalakshmi T, Prince S. Retinal model-based visual perception: applied for medical image processing. Biol InspirCogn Archit. 2016;18:95–104.

[6] O.Roopa Devi, C.Shoba BindhuIdentification of Glaucoma using deep learning: A systematic literature review, 19-21 December 2024.

[7] A. A. Salam, T. Khalil, M.U. Akram, A. Jameel and I. Basit, “Automated detection of glaucoma using structural and non structural features,” Springerplus, vol. 5, pp. 1–22, 2016.

[8] Chan EW, Li X, Tham Y-C, Liao J, Wong TY, Aung T, Cheng C-Y. Glaucoma in asia: regional prevalence variations and future projections. Br J Ophthalmol. 2016;100(1):78– 85.

[9] McMonnies CW. Glaucoma history and risk factors. J Optomet. 2017;10(2):71–8.

[10] Hu M, Zhu C, Li X, Xu Y. Optic cup segmentation from fundus images for glaucoma diagnosis. Bioengineered.2017;8(1):21–8.

[11] E. Dervisevic, S. Pavljasevic, A. Dervisevic, S.S. Kasumovic, “Challenges In Early Glaucoma Detection,” Med Arch., vol. 70, pp. 203–207, June 2016.

[12] Mitchell TM. Does machine learning really work? AI Mag. 1997;18(3):11.

[13] Cheng J, Liu J, Xu Y, Yin F, Wong DWK, Tan N-M, Tao D, Cheng C-Y, Aung T, Wong TY. Superpixel classification based optic disc and optic cup segmentation for glaucoma screening. IEEE Trans Med Imag. 2013;32(6):1019–32.

[14] Chrástek R, Wolf M, Donath K, Niemann H, Paulus D, Hothorn T, Lausen B, Lämmer R, Mardin CY, Michelson G. Automated segmentation of the optic nerve head for diagnosis of glaucoma. Med Image Anal.2005;9(4):297–314.

[15] 15. Mabuchi F, Sakurada Y, Kashiwagi K, Yamagata Z, Iijima H, Tsukahara S. Association between genetic variants associated with vertical cup-to-disc ratio and phenotypic features of primary open-angle glaucoma. Ophthalmology 2012;119(9):1819–25.

[16] Hu M, Zhu C, Li X, Xu Y. Optic cup segmentation from fundus images for glaucoma diagnosis. Bioengineered 2017;8(1):21–8.

[17] Jonas JB, Bergua A, Schmitz-Valckenberg P, Papastathopoulos KI, Budde WM. Ranking of optic disc variables for detection of glaucomatous optic nerve damage. Investing Ophthalmol Visual Sci. 2000;41(7):1764–73.

[18] Issac A, Sarathi MP, Dutta MK. An adaptive threshold based image processing technique for improved glaucoma detection and classification. Comput Methods Prog Biomed. 2015;122(2):229–44.

[19] Singh A, Dutta MK, ParthaSarathi M, Uher V, Burget R. Image processing based automatic diagnosis of glaucoma using wavelet features of segmented optic disc from fundus image. Comput Methods Prog Biomed.2016;124:108–20.

[20] Maheshwari S, Pachori RB, Kanhangad V, Bhandary SV, Acharya UR. Iterative variational mode decomposition based automated detection of glaucoma using fundus images. Comput Biol Med. 2017;88:142–9.

[21] Koh JE, Ng EY, Bhandary SV, Hagiwara Y, Laude A, Acharya UR. Automated retinal health diagnosis using pyramid histogram of visual words and fisher vector techniques. Computers in biology and medicine. 2018;92:204–9.

[22] Mohamed NA, Zulkifley MA, Zaki WMDW, Hussain A. An automated glaucoma screening system using cup-to-disc ratio via simple linear iterative clustering superpixel approach. Biomed Signal Process Control. 2019;53:101454.

[23] Rehman ZU, Naqvi SS, Khan TM, Arsalan M, Khan MA, Khalil M. Multi-parametric optic disc segmentation using superpixel based feature classification. Expert Syst Appl. 2019;120:461–73.

[24] X. Chen, Y. Xu, D. W. K. Wong, T. Y. Wong, and J. Liu, “Glaucoma detection based on deep convolutional neural network,” in 2015 37th annual international conference of the IEEE engineering in medicine and biology society (EMBC). IEEE, 2015, pp. 715–718.

[25] H.S. Alghamdi, H.L. Tang, S.A. Waheeb, T. Peto, “Automatic Optic Disc Abnormality Detection in Fundus Images: A Deep Learning Approach,” OMIA3 (MICCAI 2016), pp. 10–17, Athens, October 2016.

[26] Q. Abbas, “Glaucoma-deep: detection of glaucoma eye disease on retinal fundus images using deep learning,” Int J Adv Comput Sci Appl, vol. 8,no. 6, pp. 41–5, 2017.

[27] Yidong Chai, Hongyan Liu, Jie Xu, “Glaucoma Diagnosis Based on Both Hidden Features and Domain Knowledge through Deep Learning Models”, S0950-7051(18)30394-0. 2018,knowledge based system

[28] Chai Y, Liu H, Xu J. Glaucoma diagnosis based on both hidden features and domain knowledge through deep learning models. Knowl-Based Syst. 2018;161:147–56.

[29] Sertan Serte, Ali Serener, “A Generalized deep learning model for glaucoma detection”, 978-1-7281-3789-6/19/ 2019 IEEE

[30] Shuang Yu, Di Xiao, Shaun Frost, YogesanKanagasingam, “Robust Optic Disc and Cup Segmentation with Deep Learning for Glaucoma Detection”, S0895-6111(18)30557-3. 2019,Computerized medical Image Graphics.

[31] M. Claro, L. Santos, W. Silva Fl´avio Ara´ujo, N. Moura, “Automatic Glaucoma Detection Based on Optic Disc Segmentation and Texture Feature Extraction,” CleiEletronic Journal, vol. 19, pp. 1–10, August 2016.

[32] Y. Hagiwara, J. E. W. Koh, J. H. Tan, S. V. Bhandary, A. Laude, E. J. Ciaccio, L. Tong, and U. R. Acharya, "Computer-aided diagnosis of glaucoma using fundus images: A review," Computer methods and programs in biomedicine, vol. 165, pp. 1–12, 2018.

[33] Son J, Shin JY, Kim HD, Jung K-H, Park KH, Park SJ. Development and validation of deep learning models for screening multiple abnormal findings in retinal fundus images. Ophthalmology. 2019;127(1):85–94.

[34] Zhu C, Zou B, Zhao R, Cui J, Duan X, Chen Z, Liang Y. Retinal vessel segmentation in colour fundus images using extreme learning machine. Comput Med Imag Graph. 2017;55:68–77.

[35] T. Saba, S. T. F. Bokhari, M. Sharif, M. Yasmin, M. Raza, Fundus image classification methods for the detection of glaucoma: A review, Microsc. Res. Tech., 81 (2018), 1105–1121.

[36] Abdullah Sarhan, Jon Rokne, Reda Alhajj , "Glaucoma Detection using Image Processing Techniques: A Literature Review", CDATA(2019) S0895-6111(19)30075-8.

[37] Daniele M. S. Barros, Julio C. C. Moura1, Cefas R. Freire, Alexandre C. , Ricardo A. M. Valentim and Philippi S. G. Morais, " Machine learning applied to retinal image processing for glaucoma detection: review and perspective", biomedical engg. Online (2020),19:20.

[38] Amsa Shabbir1, Aqsa Rasheed, Huma Shehraz, Aliya Saleem, Bushra Zafar, Muhammad Sajid, Nouman Ali, Saadat Hanif Dar and Tehmina Shehryar," Detection of glaucoma using retinal fundus images: A comprehensive review", MBE, 18(3): 2033–2076(2021)

[39] Atalie C. Thompson, Alessandro A. Jammal, and Felipe A.Medeiros, "A Review of Deep Learning for Screening, Diagnosis, and Detection of Glaucoma Progression", tvst.arvojournals.org | ISSN: 2164-2591(2020)

[40] Syna Sreng, NoppadolManeerat, Kazuhiko Hamamoto and Khin Yadanar Win, "Deep Learning for Optic Disc Segmentation and Glaucoma Diagnosis on Retinal Images" Appl. Sci. 2020, 10, 49176.

[41] Soheila Gheisari, Sahar Shariflou, Jack Phu, Paul J. Kennedy, Ashish Agar, Michael Kalloniatis& S. Mojtaba Golzan,"A combined convolutional and recurrent neural network for enhanced glaucoma detection", Scientific report 2021,11:1945.

[42] Aljohani, A., Aburasain, R.Y. A hybrid framework for glaucoma detection through federated machine learning and deep learning models. *BMC Med Inform Decis Mak* **24**, 115 (2024). https://doi.org/10.1186/s12911-024-02518-y

[43] Shajila Beegam M K & Mala Kalra. (2024) Leveraging CNN and Fundus Imaging for Enhanced Glaucoma Detection. *SN Computer Science* 5:8.

Citation: S. N. Nisha Rani, R. Nagadeepa, P. Jebane, M. Elayaraja. (2025). A Two-Stage Deep Learning Framework for Automated Glaucoma Detection Using U-Net and CNN Ensembles. International Journal of Electronics and Communication Engineering and Technology (IJECET), 16(2), 36–59.

Abstract Link: https://iaeme.com/Home/article_id/IJECET_16_02_003

Article Link:
https://iaeme.com/MasterAdmin/Journal_uploads/IJECET/VOLUME_16_ISSUE_2/IJECET_16_02_003.pdf

✉ **editor@iaeme.com**